

Domain Walls in QCD

Michael McNeil Forbes and Ariel R. Zhitnitsky

Department of Physics and Astronomy, University of British Columbia, Vancouver, BC V6T 1Z1, Canada

QCD was shown to have a nontrivial vacuum structure due to the topology of the $\theta \equiv \theta + 2\pi n$ parameter. As a result of this nontrivial topology, quasi-stable QCD domain walls appear characterized by a transition in the singlet η' field. We discuss the physics of these QCD domain walls as well as related axion domain walls and we present a new type of axion wall which also contains an η' transition. We argue that QCD domain walls, though classically stable, are unstable on the quantum level due to tunneling. Their lifetime is short enough that no cosmic QCD domain walls remain today, however, it is long enough that QCD domain walls could play an important role in the evolution of early universe. They may also be detectable in energetic collisions such as those at the Relativistic Heavy Ion Collider (RHIC).

I. INTRODUCTION

Color confinement, spontaneous breaking of chiral symmetry, the $U(1)$ problem, θ dependence, and the classification of vacuum states are some of the most interesting questions in QCD. Unfortunately, the progress in our understanding of them is extremely slow. At the end of the 1970s A. M. Polyakov [1] demonstrated color confinement in 3-dimensional QED (QED₃): this was the first example in which nontrivial dynamics of the ground state played a key role. Many papers were written regarding the ground state structure of gauge theories in the strong coupling regime, but there were many unanswered questions. Almost 20 years passed before the next important piece of the puzzle was solved [2]. Seiberg and Witten demonstrated that confinement occurs in supersymmetric (SUSY) QCD₄ due to the condensation of monopoles: a similar mechanism was suggested many years ago by 't Hooft and Mandelstam (see [3] for a review). Furthermore, condensation of dyons together with oblique confinement for nonzero vacuum angle θ was also discovered in SUSY models [4] (this phenomenon was also argued to take place in ordinary QCD. See [3]).

In addition to providing solid demonstration of earlier ideas, the recent progress in SUSY models has introduced many new phenomena, such as the existence of rich vacuum state structure and the existence of domain walls [5]: topologically stable interpolations connecting the same vacuum state. The same conclusion was reached by Witten in [6] based on a D-brane construction in the limit of large N_c . In fact, one can see that in both approaches, the number of states in the vacuum family is N_c . Motivated by this development in SUSY gauge theories D-brane construction, we ask how this applies to QCD. The issue of classifying the vacuum states for a given parameter θ as well as the phenomenological consequences (domain walls and their decay etc.) is the subject of this work. In separate publications [7] we shall apply these results to analyze the physics after the QCD phase transition in evolution of early Universe. In particular, we discuss the possibility of generation of primordial magnetic fields due to the existence of short-lived QCD domain walls discussed in this paper.

The starting point of our analysis is an effective Lagrangian approach. Experience with SUSY models demonstrates that the effective Lagrangian approach is a very effective tool for the analysis of large distance dynamics in the strong coupling regime. There are two different definitions of an effective Lagrangian in quantum field theory. One of them is the Wilsonian effective Lagrangian describing the low energy dynamics of the lightest particles in the theory. In QCD, this is implemented by effective chiral Lagrangians for the pseudoscalar mesons. Another type of effective Lagrangian is defined by taking the Legendre transform of the generating functional for connected Green's functions to obtain an effective potential. This object is useful in addressing questions about the vacuum structure of the theory in terms of vacuum expectation values (VEVs) of composite operators—these VEVs minimize the effective action. The latter approach is well suited for studying the dependence of the vacuum state on external parameters such as the light quark masses or the vacuum angle θ . However, it is not, for example, useful for studying S -matrix elements because the kinetic term cannot be recovered through this approach. The utility of the second approach for gauge theories had been recognized long ago for supersymmetric models, where the anomalous effective potential was found for both the pure supersymmetric gluodynamics [8] and supersymmetric QCD (SQCD) [9] models. Properties of the vacuum structure in the SUSY models were correctly understood only after analyzing this kind of effective potential.

This paper contains many of the details mentioned in the letter [7] and is organized as follows:

Section II: Here we review the properties of the QCD effective Lagrangian [10] which is a generalization of the Di Vecchia-Veneziano-Witten (VW) Lagrangian [11] to include terms subleading in $1/N_c$ as well as to account

for a constraint due to the quantization topological charge¹. One should emphasize from the very beginning that the specific form of the effective potential used in this paper is not critical for the present analysis: only the topological structure and winding $\theta \rightarrow \theta + 2\pi n$ —a consequence of the topological charge quantization—is essential.

Section III: This is devoted to the analysis of different types of the domain walls (exclusively QCD domain walls, as well as the axion domain walls) which are classically stable due to the topological consideration.

Section IV: Here we argue the QCD domain walls are not stable on the quantum level due to a tunneling phenomena. We estimate their lifetime which is macroscopic, but short on a cosmological scale. Thus, these domain walls are not a cosmological problem, in fact, they may be quite useful in the sense that the short-lived domain walls may play an important role in forming primordial magnetic fields as suggested in [7].

Section V: This is our conclusion.

II. EFFECTIVE LAGRANGIAN AND θ DEPENDENCE IN QCD

Our analysis begins with the effective low energy QCD action derived in [10], which allows the θ -dependence of the ground state to be analyzed. Within this approach, the pseudo-Goldstone fields and η' field are described by the unitary matrix U_{ij} , which correspond to the γ_5 phases of the chiral condensate: $\langle \bar{\Psi}_L^i \Psi_R^j \rangle = -|\langle \bar{\Psi}_L \Psi_R \rangle| U_{ij}$ with

$$U = \exp \left[i\sqrt{2} \frac{\pi^a \lambda^a}{f_\pi} + i \frac{2}{\sqrt{N_f}} \frac{\eta'}{f_{\eta'}} \right], \quad UU^\dagger = 1, \quad (1)$$

where λ^a are the Gell-Mann matrices of $SU(N_f)$, π^a is the pseudoscalar octet, and $f_\pi = 133$ MeV. In terms of U the low-energy effective potential is given by [10]:

$$W_{\text{QCD}}(\theta, U) = - \lim_{V \rightarrow \infty} \frac{1}{V} \log \sum_{l=0}^{N_c-1} \exp \left\{ VE \cos \left(-\frac{\theta}{N_c} + i \frac{1}{N_c} \log \text{Det } U + \frac{2\pi}{N_c} l \right) + \frac{1}{2} V \text{Tr} (MU + M^\dagger U^\dagger) \right\}. \quad (2)$$

All dimensional parameters in this potential are expressed in terms of the QCD vacuum condensates, and are well known: $M = \text{diag}(m_q^i |\langle \bar{\Psi}^i \Psi^i \rangle|)$; and the constant E is related to the QCD gluon condensate $E = \langle \frac{b\alpha_s}{32\pi} G^2 \rangle$, where numerically $3b = 11N_c - 2N_f$; quark condensate $\langle \bar{\Psi}^i \Psi^i \rangle \simeq -(240 \text{ MeV})^3$, gluon condensate $\langle \frac{\alpha_s}{\pi} G^2 \rangle \simeq 1.2 \times 10^{-2} \text{ GeV}^4$.

It is possible to argue that equation (2) represents the anomalous effective Lagrangian realizing broken conformal and chiral symmetries of QCD. The arguments are that Equation (2):

1. correctly reproduces the VVW effective chiral Lagrangian, [11] in the large N_c limit
[For small values of $(\theta - i \log \text{Det } U)$, the term with $l = 0$ dominates the infinite volume limit. Expanding the cosine (this corresponds to the expansion in $1/N_c$), we recover exactly the VVW effective potential [11] together with the constant term $-E = -\langle b\alpha_s/(32\pi)G_{\mu\nu}^2 \rangle$ required by the conformal anomaly:

$$W_{VVW}(\theta, U, U^\dagger) = -E - \frac{\langle \nu^2 \rangle_{YM}}{2} (\theta - i \log \text{Det } U)^2 - \frac{1}{2} \text{Tr} (MU + M^\dagger U^\dagger) + \dots, \quad (3)$$

here we used the fact that at large N_c , $E/N_c^2 = -\langle \nu^2 \rangle_{YM}$ is the topological susceptibility in pure YM theory. Corrections in $1/N_c$ stemming from Equation (2) constitute a new result of [10].

2. reproduces the anomalous conformal and chiral Ward identities of QCD,
[Let us check that the anomalous Ward Identities (WI's) in QCD are reproduced from Equation (2). The anomalous chiral WI's are automatically satisfied with the substitution $\theta \rightarrow (\theta - i \log \text{Det } U)$ for any N_c , in accord with [11]. Furthermore, it can be seen that the anomalous conformal WI's of [13] for zero momentum correlation functions of the operator $G_{\mu\nu}^2$ in the chiral limit $m_q \rightarrow 0$ are also satisfied when E is chosen as above. As another important example of WI's, the topological susceptibility in QCD near the chiral limit will

¹Such a generalization was also motivated by SUSY consideration [12], see also [5] for a review.

be calculated from Equation (2). For simplicity, the limit of $SU(N_f)$ isospin symmetry with N_f light quarks, $m_q \ll \Lambda_{\text{QCD}}$ will be considered. For the vacuum energy for small θ one obtains [10]

$$E_{\text{vac}}(\theta) = -E + m_q \langle \bar{\Psi} \Psi \rangle N_f \cos\left(\frac{\theta}{N_f}\right) + \mathcal{O}(m_q^2) . \quad (4)$$

Differentiating this expression twice with respect to θ reproduces the chiral Ward identities [14]:

$$\lim_{q \rightarrow 0} i \int dx e^{iqx} \langle 0 | T \left\{ \frac{\alpha_s}{8\pi} G \tilde{G}(x) \frac{\alpha_s}{8\pi} G \tilde{G}(0) \right\} | 0 \rangle = -\frac{\partial^2 E_{\text{vac}}(\theta)}{\partial \theta^2} = \frac{1}{N_f} m_q \langle \bar{\Psi} \Psi \rangle + \mathcal{O}(m_q^2) . \quad (5)$$

Other known anomalous WI's of QCD can be reproduced from Equation (2) in a similar fashion. Consequently, Equation (2) reproduces the anomalous conformal and chiral Ward identities of QCD, and in this sense passes the test for it to be the effective anomalous potential for QCD.]

3. reproduces the known results for the θ dependence [11].

[As mentioned earlier, our results are similar to those found in [11]. A new element which was not discussed in 80's, is the procedure of summation over l in (2). As we shall discuss in a moment, this leads to the cusp structure of the effective potential which seems to be an unavoidable consequence of the topological charge quantization². These singularities are analogous to the ones arising in SUSY models and show the non-analyticity of phases at certain values of θ . The origin of this non-analyticity is clear, it appears when the topological charge quantization is imposed explicitly at the effective Lagrangian level.]

An interesting note is that, in general, the θ dependence appears in the combination θ/N_c , (see equation (2)) which naïvely does not provide the desired 2π periodicity for the physical observables; equation (2), however, explicitly demonstrates the 2π periodicity of the partition function. This seeming contradiction is resolved by noting that in the thermodynamic limit, $V \rightarrow \infty$, only the term of lowest energy in the summation over l is retained for a particular value of θ , creating the illusion of θ/N_c periodicity in the observables. Of course, the values θ and $\theta + 2\pi$ are physically equivalent for the entire set of states, but relative transitions—switching branches—between different θ states have physical significance. Exactly this important property will be used in what follows for the construction of the domain walls which are classically stable, non-trivial interpolations between physically equivalent vacuum states (see below). Consequently, the θ dependence in the infinite volume limit appearing in the combination θ/N_c is a result of being stuck in a particular state: The local geometry give the impression of θ/N_c periodicity but the topology gives the true θ periodicity. The reader is referred to the original papers [10] for more detailed discussions of the properties of the effective potential (2).

Our final remark regarding (2). The appearance of the cosine interaction, $\cos(\theta/N_c)$, implies³ the following scenario in pure gluodynamics (ϕ_i 's frozen): the $(2k)^{\text{th}}$ derivative of the vacuum energy with respect to θ , as $\theta \rightarrow 0$, is expressed solely in terms of one parameter, $\frac{1}{N_c}$, for arbitrary k :

$$\left. \frac{\partial^{2k} E_{\text{vac}}(\theta)}{\partial \theta^{2k}} \right|_{\theta=0} \sim \int \prod_{i=1}^{2k} d^4 x_i \langle Q(x_1) \dots Q(x_{2k}) \rangle \sim \left(\frac{i}{N_c} \right)^{2k} , \quad (6)$$

where, $Q = \frac{\alpha_s}{8\pi} G \tilde{G}$. This property was seen as a consequence of Veneziano's solution of the $U(1)$ problem [15]. The reason that only one factor appears in Veneziano's calculation is that the corresponding correlation function, $\sim \int \prod_{i=1}^{2k} d^4 x_i \langle Q(x_1) \dots Q(x_{2k}) \rangle$, becomes saturated at large distances by the Veneziano ghosts whose contributions factorize exactly, and was subsequently interpreted as a manifestation of the θ/N_c dependence in gluodynamics at small θ . However, at that time it was incorrectly assumed that such a dependence indicates that the periodicity in θ is proportional to $2\pi N_c$. We now know that the standard 2π periodicity in gluodynamics is restored by the summation over l in (2) such that one jumps from one branch to another at $\theta = \pi$.

²this element was not explicitly imposed in the approach of [11]; the procedure was suggested much later to cure some problems in SUSY models [12] and references therein; analogous construction was discussed for gluodynamics and QCD in [10].

³As we noticed in the introduction, the specific form of the potential is not very essential for what follows. However, this form is very appealing for the present study because with it, we can describe some of the domain walls in the analytical form (see below, for example (26)).

In the next section we shall discuss different types of domain walls which interpolate between various vacuum states, but first we should study the classification of vacuum states themselves. In order to do so, it is convenient to parameterize the fields U as

$$U = \begin{pmatrix} e^{i\phi_1} & 0 & \cdots & 0 \\ 0 & e^{i\phi_2} & \cdots & 0 \\ \vdots & \vdots & \ddots & 0 \\ 0 & 0 & 0 & e^{i\phi_{N_f}} \end{pmatrix} \quad (7)$$

such that the potential (2) takes the form

$$V(\phi_i, \theta) = -E \cos \left(\frac{1}{N_c} \theta - \frac{1}{N_c} \sum \phi_i \right) - \sum M_i \cos \phi_i. \quad (8)$$

The minimum of this potential is determined by the following equation:

$$\frac{1}{N_c} \sin \left(\frac{1}{N_c} \theta - \frac{1}{N_c} \sum \phi_i \right) = \frac{M_i}{E} \sin \phi_i, \quad i = 1, \dots, N_f. \quad (9)$$

At lowest order in $1/N_c$ this equation coincides with that of [11]. For general values of M_i/E , it is not possible to solve Equation (9) analytically, however, in the realistic case $\varepsilon_u, \varepsilon_d \ll 1$, $\varepsilon_s \sim 1$ where $\varepsilon_i = \frac{N_c M_i}{E}$, the approximate solution can be found:

$$\begin{aligned} \sin \phi_u &= \frac{m_d \sin \theta}{[m_u^2 + m_d^2 + 2m_u m_d \cos \theta]^{1/2}} + O(\varepsilon_u, \varepsilon_d), \\ \sin \phi_d &= \frac{m_u \sin \theta}{[m_u^2 + m_d^2 + 2m_u m_d \cos \theta]^{1/2}} + O(\varepsilon_u, \varepsilon_d), \\ \sin \phi_s &= O(\varepsilon_u, \varepsilon_d). \end{aligned} \quad (10)$$

This solution coincides with the one of [11] to leading order in $\varepsilon_u, \varepsilon_d$. In what follows for the numerical estimates and for simplicity we shall use the $SU(2)$ limit $m_u = m_d \ll m_s$ where the solution (10) can be approximated as:

$$\begin{aligned} \phi_u &\simeq \frac{\theta}{2}, \quad \phi_d \simeq \frac{\theta}{2}, \quad \phi_s \simeq 0, \quad 0 \leq \theta < \pi, \\ \phi_u &\simeq \frac{\theta + 2\pi}{2}, \quad \phi_d \simeq \frac{\theta - 2\pi}{2}, \quad \phi_s \simeq 0, \quad \pi \leq \theta < 2\pi, \quad \text{etc.} \end{aligned} \quad (11)$$

Once solution (11) is known, one can calculate the vacuum energy and topological charge density $Q = \langle 0 | \frac{\alpha_s}{8\pi} G\tilde{G} | 0 \rangle$ as a function of θ . In the limit $m_u = m_d \equiv m$, $\langle \bar{d}d \rangle = \langle \bar{u}u \rangle \equiv \langle \bar{\Psi}\Psi \rangle$ one has:

$$\begin{aligned} V_{\text{vac}}(\theta) &\simeq V_{\text{vac}}(\theta = 0) + 2m |\langle \bar{\Psi}\Psi \rangle| (1 - |\cos \frac{\theta}{2}|) \\ \langle \theta | \frac{\alpha_s}{8\pi} G\tilde{G} | \theta \rangle &= -\frac{\partial V_{\text{vac}}(\theta)}{\partial \theta} = -m |\langle 0 | \bar{\Psi}\Psi | 0 \rangle| \sin \frac{\theta}{2}. \end{aligned} \quad (12)$$

As expected, the θ dependence appears only in combination with m and goes away in the chiral limit. One can also calculate the chiral condensate $\langle \bar{\Psi}_L^i \Psi_R^i \rangle$ in the θ vacua using solution (11) for vacuum phases:

$$\langle \theta | \bar{\Psi}\Psi | \theta \rangle = \cos \frac{\theta}{2} \langle 0 | \bar{\Psi}\Psi | 0 \rangle_{\theta=0}, \quad \langle \theta | \bar{\Psi} i \gamma_5 \Psi | \theta \rangle = -\sin \frac{\theta}{2} \langle 0 | \bar{\Psi}\Psi | 0 \rangle_{\theta=0} \quad (13)$$

Two remarks are in order. First of all, as is known, in the infinite volume limit and in thermal equilibrium the $|\theta\rangle$ vacuum state is the absolutely stable ground state of a different world with physics quite different from our own. In particular, P and CP symmetries are strongly violated in this world due to, for example, non-zero values of P and CP violating condensates (12,13). In spite of the fact that the $|\theta\rangle$ vacuum state has a higher energy (12), this state is stable due to the following superselection rule: There is no gauge invariant observable \mathcal{A} in QCD, which can communicate between different θ states, $\langle \theta' | \mathcal{A} | \theta \rangle \sim \delta(\theta - \theta')$. Therefore, there are no transitions between these states [16]. The problem of why $\theta = 0$ in our world is known as the strong CP problem. Our best solution to this problem, which has been known for many years, is to introduce the Peccei-Quinn symmetry [17] and the corresponding pseudo-goldstone

particle known as the axion [18–21]. The axion solution to the strong CP problem suggests that the θ parameter of QCD be promoted to a dynamical axion field $\theta \rightarrow \frac{a(x)}{f_a}$ with very small coupling constant, $1/f_a \ll 1$. Once θ becomes a dynamical field, it automatically relaxes to $\theta = 0$ as the lowest energy state of (12). In the following we shall study different types of domain walls: Axion domain walls where θ is the dynamical axion field and QCD domain walls where θ is the fundamental parameter of the theory which is fixed in our world to $\theta = 0$.

Our second remark is more technical, but critical to an understanding of the QCD domain walls. Physically, the states $\theta = 0$ and $\theta = 2\pi n$ are identical: they represent the *same* state. However, as one can see from Equation (11), the solutions for the ground states corresponding to $\theta = 0$ and $\theta = 2\pi$ are not described in the same way: $\theta = 0$ corresponds to $\phi_u = \phi_d = 0$ while $\theta = 2\pi$ corresponds to $\phi_u = 2\pi$, $\phi_d = 0$. It is clear that the physics in both these states is exactly the same: If we lived in one of these states and ignored the others, then we could assign an arbitrary phase $\sim 2\pi n$ for each ϕ_u or ϕ_d separately and independently. However, if we want to interpolate between these states to get feeling about both of them, the difference in phases between these states can no longer be a matter of choice, but rather is specified by Equation (11). This classification arises because the singlet combination $\phi_S = \sum \phi_i$ really lives on a $U(1)$ manifold which is a circle. The integer n is only important if we are discussing transitions around the $U(1)$ circle: in this case, it is important to keep track of how many times you wind around the center. Thus, n is a topological winding number which plays an important role when the physics can interpolate around the entire $U(1)$ manifold. We illustrate this idea in Figure 1. Here, we show three topologically distinct paths in a two-dimensional space with an impenetrable barrier in the center. The paths that wind around the barrier cannot be deformed into the other paths. Each path is characterized by a winding number n .

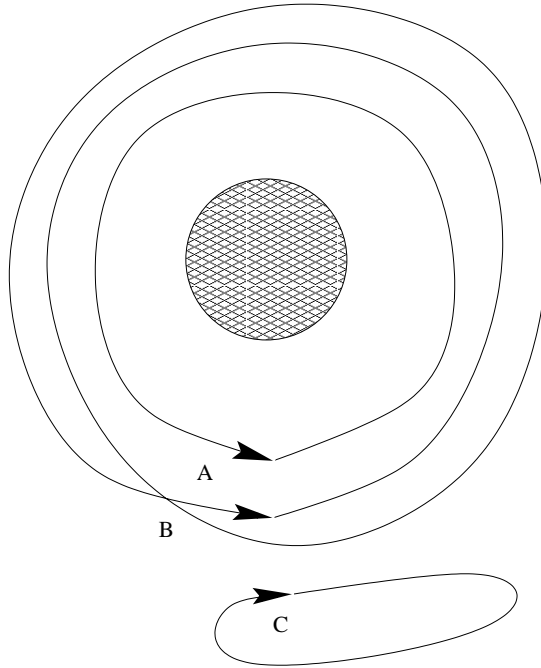


FIG. 1. Three examples of transitions that are topologically different. Paths A and B wind around the hole once ($n = 1$) and twice ($n = 2$) respectively whereas path C does not wind ($n = 0$). Path C can be shrunk to a point whereas the others cannot. Each path is said to belong to a different homotopy class. Only paths A and B are affected by the topology of the space. Path C might imagine that it is living in a space with no hole.

In the notation of Equation (11), the windings are interpreted as interpolations from one state to another: Each state is identical if there is no means of interacting with the other states but, once interpolations (windings) are discussed, all of the states must be considered. In this case the relative separation (winding) of the interacting states is critical. Both of these pictures are valid. Thus, when we discuss the vacuum states $\theta = 0$ corresponding to $\phi_u = \phi_d = 0$ and $\theta = 2\pi$ corresponding to $\phi_u = 2\pi$, $\phi_d = 0$, we are really anticipating a transition around the $U(1)$ circle (a domain wall) which will link these “two” states.

At this point, one can forget about the external θ parameter (which was essentially a helpful tool in analysis of the structure of the different vacuum states) and put $\theta = 0$ as it is in our world. A nontrivial field configuration winding around the $U(1)$ manifold can be entirely expressed in terms of the ϕ_u and ϕ_d phases with $\theta = 0$ fixed. In terms of physical fields this transition corresponds to the interpolation of the π^0 , η , and η' physical fields. We refer

to this type of transition as a QCD domain wall (see Section III B). If we accept the axion solution to the strong CP problem, then θ becomes a relevant degree of freedom in the transitions. We refer to transitions involving a transition the dynamical axion field as axion domain walls (see Section III C). One should note that in SUSY models (with soft breaking terms), different types of domain walls were extensively studied in the literature, see [22], [23], and for a review, [5]. In QCD, an analysis for the similar domain walls interpolating between different *non-degenerate* physical states was carried out in [24]. Such domain walls were designed to describe a decay of metastable vacua (which exist for certain ranges of parameters). We will *not* discuss such kinds of domain walls in this paper.

A closest analogue of the situation described above is the well-known $2D$ sine-Gordon model defined by the Lagrangian $L = \frac{1}{2}(\partial_\mu \phi)^2 - \lambda \cos(\phi)$. In this case the shift $\phi \rightarrow \phi + 2\pi n$ is a symmetry of the Lagrangian emphasizing the underlying $U(1)$ nature of the solution manifold: the corresponding homotopy group π_0 is nontrivial. As is known, this leads to important consequences such as an existence of a stable kink solution in two dimensions, which cannot be recovered by the standard methods of quantum field theory when one starts from the vacuum state $\langle \phi \rangle = 0$ and ignores the topology. In our case an analogous symmetry is realized by the procedure of summation over l in equation (2), which makes symmetry $\theta \rightarrow \theta + 2\pi n$ explicit. Besides that, we discuss four dimensional space-time $D = 4$ rather than $D = 2$; therefore, we expect to find a two-dimensional domain wall objects rather than the point-like objects realized in the $D = 2$ sine-Gordon model.

To better explain the idea of a topologically stable transition, we present the following example. Imagine a long thin strip of paper. Call one side A and call the ground state of the paper the state with side A facing up. If we lay the piece of paper flat, then we would say that every point is in the ground state. Now introduce a twist, returning the paper to the ground state on either side of the twist. Both the left and the right side are in their ground state, but there is a twist in the middle. We can easily remove the twist by twisting an end, but imagine that somehow the twist formed (or was already present) in an infinitely long strip⁴. There would be no way for you to remove the twist. We could describe this system by a vector pointing normal to A and expressing the angle that the vector makes with the ground state (where the vector points up) by $\phi(x)$. Note that this is redundant notation: $\phi = 0$ is equivalent to $\phi = 2\pi$ etc. To remove this redundancy and make the description smooth we can use a complex number of unit modulus. Hence, we can describe our strip at any point x by the function $u(x) = e^{i\phi(x)}$ which removes any redundancy. Now our ground state is $u(x) = 1$ everywhere and our twist is described by the transition $\phi(x) : 0 \rightarrow 2\pi$ however the true description without redundancies is $u : 1 \rightarrow 1$. Thus, $u(x)$ interpolates between two regions of the same ground state and there is no way to continuously deform $u(x)$ to remove the twist. The description of this system by a real parameter ϕ is useful, but we must implement a discrete symmetry in this picture under shifts $\phi \rightarrow \phi + 2\pi n$. It is the discrete nature of the symmetry that gives rise to the phenomena: each ground state is disconnected from the other states. The topology for the configuration space is thus not a line, but a circle and this topology has a hole. Paths which wind around the hole cannot be continuously transformed to remove the winding, and hence there different homotopy classes described by an integer n which counts the total number of windings the path makes around the hole. Associated with each n there is a topologically stable domain wall.

In the previous discussion based on the effective Lagrangian (2), we have neglected the gluon degrees of freedom. In this case, the topology of the singlet $U(1)$ field is non-trivial and windings around the singlet $U(1)$ component are absolutely stable. In reality, however, the gluon degrees of freedom are not very heavy. Thus, we must consider these extra degrees and how they affect the topology. It is the case that, when we account for the extra gluon degrees of freedom, we find that the topology is no longer that of simply $U(1)$ and in fact, the $U(1)$ loop is given a connection through the extra degrees of freedom which allows the domain walls to continuously deform to the ground state.

To see how an extra degree of freedom can change the topology, consider Figure 2. Here we have added a third dimension to show that the barrier was actually a peg of finite height. Now that we can move in the extra dimension, we can use this degree of freedom to “lift” the paths over the peg: thus, they are no longer topologically stable. In the QCD analogue, paths A and B represents domain walls (path C would be a trivial closed loop which would relax to a point representing the same vacuum state everywhere with no domain wall.). There is an energy cost to “lift” the path over the barrier and at low temperatures $T \ll \Lambda_{\text{QCD}}$ there is not enough energy to do this, so classically, the domain walls are stable. It is still possible, however, for the walls to overcome the barrier by tunneling through the barrier. The tunneling probability, however, could be low due to the height of the obstacle and hence their lifetime could be much larger than the $\Lambda_{\text{QCD}}^{-1}$ scale which could be naïvely expected for standard QCD fluctuations. See Section IV for details of the dynamics of the gluon fields.

We should also remark that with each winding, the domain wall would become more energetic. Walls with a large

⁴In Nature, such an object can be formed when the temperature was nonzero; for example, in early Universe after the QCD phase transition, or in heavy ion collisions.

number of windings would likely have enough energy to rapidly unwind, or else would separate spatially forming several domain walls of winding number ± 1 . For this reason, we discuss only the simplest walls which wind once in this paper.

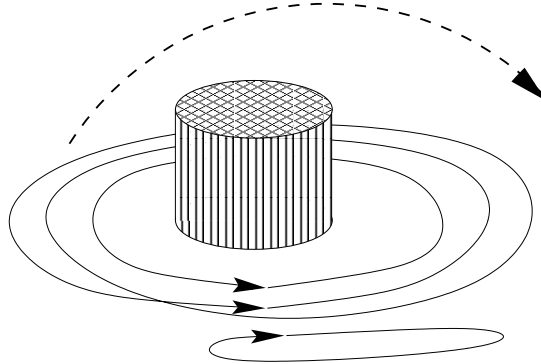


FIG. 2. Here we show the same picture as in Figure 1 except that we show the third dimension. Here we can see that all the paths are now homotopically equivalent. We can deform the paths by “lifting” them over the obstacle so that we can unwind them. If the paths were strings with some weight, then it would require some energy to “lift” the strings over the obstacle. If this energy was not available, then we would say that, classically, the configurations that wind around the peg are stable. Quantum mechanically, however, the strings could still tunnel through the peg, and so the configurations are unstable quantum mechanically. The probability that one string could tunnel into another configuration would depend on the height of the peg.

Now we return to equation (2). The effective potential (2) can be used to study the vacuum ground state (12,13) as well as the pseudo-goldstone bosons as its lowest energy excitations. In particular, one could study the spectrum as well as mixing angles of the pseudo-goldstone bosons by analyzing the quadratic fluctuations in the background field (12,13). We refer to the original papers [10,24] on the subject for details, but here we want to quote the following mass relationships for the η' meson to be used in the following discussions:

$$f_\pi^2 m_{\eta'}^2 = \frac{4N_f}{N_c^2} E + \frac{4}{N_f} \sum_{i=\{u,d,s\}} m_i |\langle 0 | \bar{\Psi}^i \Psi^i | 0 \rangle| + O(m_q^2). \quad (14)$$

This relation is in a good agreement (on the level of 20%) with phenomenology. In the chiral limit this formula takes especially simple form

$$m_{\eta'}^2 = \frac{4N_f}{f_\pi^2 N_c^2} E, \quad (15)$$

which demonstrates that, in the chiral limit, the η' mass is proportional to the gluon condensate, and is therefore related to the conformal anomaly. What is more important for us in this paper is that the combination on the right hand side of this equation exactly coincides with a combination describing the width of the QCD domain wall (see Equation (27)). For this reason, the properties of the QCD domain walls are dominated by the η' field.

III. DOMAIN WALLS

In the rest of this paper we limit ourselves with the simplest case $N_f = 2$ and neglect the difference between f_π and $f_{\eta'}$ which numerically are very close to each other. To describe the basic structure of the QCD domain walls as well as that of axion domain walls we replace the parameter θ in Equation (2) by a dynamical axion field $\theta \rightarrow N_f a = 2a$ (this corresponds to the so-called $N = 2$ axion model). We also introduce here the following dimensionless phases, ϕ_S describing the isotopical “singlet” field, and ϕ_T describing the isotopical “triplet” field. These fields correspond to the dynamical η' (singlet) and pion π^0 (triplet) fields defined in (1).

$$\phi_S = \phi_u + \phi_d, \quad \phi_T = \phi_u - \phi_d, \quad \eta' = \frac{f_\pi}{2\sqrt{2}} \phi_S, \quad \pi^0 = \frac{f_\pi}{2\sqrt{2}} \phi_T \quad (16)$$

In what follows we also need to know the masses of the relevant fields in terms of parameters of the effective potential (2):

$$m_\pi^2 = \frac{4M}{f_\pi^2}; \quad m_a^2 = \frac{4M}{f_a^2} (1 - \xi^2); \quad m_{\eta'}^2 = \frac{8}{N_c^2 f_\pi^2} E + \frac{4M}{f_\pi^2}, \quad (17)$$

where mass relation for η' follows from (14) with $N_f = 2$. Here we have neglected all possible mixing terms, and have introduced the following notations

$$M \equiv \frac{M_u + M_d}{2} = \frac{m_u |\langle 0 | \bar{\Psi}_u \Psi_u | 0 \rangle| + m_d |\langle 0 | \bar{\Psi}_d \Psi_d | 0 \rangle|}{2}, \quad \xi = \frac{M_d - M_u}{M_d + M_u} \approx 0.3. \quad (18)$$

A. Domain Wall Equations

To study the structure of the domain wall we look at a simplified model where one half of the universe is in one ground state and the other half is in another. The fields will orient themselves in such a way as to minimize the energy density in space, forming a domain wall between the two regions. In this model, the domain walls are planar and we shall neglect the x and y dimensions for now. Thus, a complete description of the wall is given by specifying the boundary conditions and by specifying how the fields vary along z .

The energy density of a domain wall is given by the following expression

$$\sigma = \int_{-\infty}^{\infty} \left(\frac{f_a^2}{4} \dot{a}^2 + \frac{f_\pi^2}{16} \dot{\phi}_T^2 + \frac{f_\pi^2}{16} \dot{\phi}_S^2 + V(\phi_S, \phi_T, a) - V_{\min} \right) dz \quad (19)$$

where the first three terms are the kinetic contribution to the energy and the last term is the potential. The kinetic term is actually a four divergence, but we have assumed the wall to be a stationary solution—hence the time derivatives vanish—and symmetric in the x - y plane. The only dependence remaining is the z dependence. Here, a dot signifies differentiation with respect to z : $\dot{a} = \frac{da}{dz}$.

Now, to find the form of the domain walls, it is convenient to use a form of the potential which follows from (8):

$$V(\phi_S, \phi_T, a) = -2M \left(\cos\left(\frac{\phi_T}{2}\right) \cos\left(\frac{\phi_S}{2} + a\right) + \xi \sin\left(\frac{\phi_T}{2}\right) \sin\left(\frac{\phi_S}{2} + a\right) \right) - E \cos\left(\frac{\phi_S}{N_c}\right). \quad (20)$$

Here we have redefined the fields $\phi_u \rightarrow \phi_u + a$ and $\phi_d \rightarrow \phi_d + a$ in order to remove the axion field from the last term $\sim E$ and to insert it into the term $\sim M$. To minimize these equations, we can apply a standard variational principle and arrive at the following equations of motion for the domain wall solutions:

$$\frac{\ddot{a} f_a^2}{4M} = \cos\left(\frac{\phi_T}{2}\right) \sin\left(\frac{\phi_S}{2} + a\right) - \xi \sin\left(\frac{\phi_T}{2}\right) \cos\left(\frac{\phi_S}{2} + a\right), \quad (21)$$

$$\frac{\ddot{\phi}_T f_\pi^2}{8M} = \sin\left(\frac{\phi_T}{2}\right) \cos\left(\frac{\phi_S}{2} + a\right) - \xi \cos\left(\frac{\phi_T}{2}\right) \sin\left(\frac{\phi_S}{2} + a\right), \quad (22)$$

$$\frac{\ddot{\phi}_S f_\pi^2}{8M} = \cos\left(\frac{\phi_T}{2}\right) \sin\left(\frac{\phi_S}{2} + a\right) - \xi \sin\left(\frac{\phi_T}{2}\right) \cos\left(\frac{\phi_S}{2} + a\right) + \frac{E}{MN_c} \sin\left(\frac{\phi_S}{N_c}\right), \quad (23)$$

where the last term of equation (23) should be understood as the lowest branch of the multivalued function described by equation (2). Namely, for $\phi_S \notin [0, \pi]$, this should be interpreted as $\sin(\frac{\phi_S - 2\pi l}{N_c})$ with the integer l chosen to minimize the potential term $\cos \frac{\phi_S - 2\pi l}{N_c}$. For example, with $\pi \leq \phi_S \leq 2\pi$, the last term should be of the form $\sin(\frac{\phi_S - 2\pi}{N_c})$.

Notice the following features: first, the trigonometric terms on the right hand side are of, at most, order 1; thus the scale for the curvature (or rather, the second derivative) of the domain wall solutions is limited by f_a^2/M and f_π^2/M etc. In particular, the axion domain wall must have a characteristic scale larger than $m_a^{-1}/(1 - \xi^2)$ and the pion domain wall must have a scale larger than m_π^{-1} . The last term in equation governing the ϕ_S field can potentially be somewhat larger than 1, hence the smallest scale for the ϕ_S field is related to the η' mass. We see immediately that an axion domain wall must have a structure some thirteen orders of magnitude larger than the natural QCD scale and that the η' field can have structure one order of magnitude smaller than that of the pion field.

B. QCD Domain Walls

Here we consider the most important case of the QCD domain wall solution which exists with or without an axion field. So we now set $a = 0$. The equations of motion become:

$$\begin{aligned}\frac{\ddot{\phi}_T f_\pi^2}{8M} &= \sin\left(\frac{\phi_T}{2}\right) \cos\left(\frac{\phi_S}{2}\right) - \xi \cos\left(\frac{\phi_T}{2}\right) \sin\left(\frac{\phi_S}{2}\right), \\ \frac{\ddot{\phi}_S f_\pi^2}{8M} &= \cos\left(\frac{\phi_T}{2}\right) \sin\left(\frac{\phi_S}{2}\right) - \xi \sin\left(\frac{\phi_T}{2}\right) \cos\left(\frac{\phi_S}{2}\right) + \frac{E}{MN_c} \sin\left(\frac{\phi_S}{N_c}\right).\end{aligned}\quad (24)$$

For convenience, we shall label the vacuum states using the notation (ϕ_u, ϕ_d) . Thus, we have only one physical ground state $(\phi_u, \phi_d) = (0, 0)$, however, because of topology of the $U(1)$ component of the fields, described near the end of Section II, classically stable domain walls can form and interpolate from the ground state $(\phi_u, \phi_d) = (0, 0)$ along a path which is not homotopic to the null path. To classify the homotopic paths we use the redundant notation where $(0, 0)$ and $(2\pi, 0)$ etc. are considered as different states and we talk about the field interpolating between these states. Keep in mind that this is only a way of classifying the homotopy classes and that in fact all the states represented by $(2\pi n, 2\pi m)$ for integers m and n are one in the same vacuum state.

The simplest classically stable path which is homotopically distinct from the null path is classified by a continuous transition from $(\phi_u, \phi_d) = (0, 0)$ the same ground state labeled $(\phi_u, \phi_d) = (2\pi, 0)$ described by the vacuum solution Equation (11) with $\theta = 2\pi$ (or, equivalently, $l = -1$ in Equation (2)). We emphasize once again that $\theta = 2\pi$ is equivalent to $\theta = 0$, however, the vacuum solution $(\phi_u, \phi_d) = (2\pi, 0)$ represents a different branch, $l = -1$ in Equation (2). The importance of the choice of branch comes when a transition is made from one branch to another: in this case, the first ground state is in the branch $l = 0$ and the second is in the branch $l = -1$. Thus, the wall winds once around the $U(1)$ circle. It is also possible to wind in the opposite sense. To summarize, the two topologically stable domain walls of minimal energy correspond one winding in each direction and are classified by the transitions from $(\phi_u, \phi_d) = (0, 0)$ to:

Soliton $(\phi_u, \phi_d) = (2\pi, 0)$.

Antisoliton $(\phi_u, \phi_d) = (-2\pi, 0)$.

Note, that in the chiral limit $m_u = m_d$ and $\xi = 0$, thus the transitions to $(\phi_u, \phi_d) = (0, \pm 2\pi)$ has the same energy and there is a degeneracy. If $m_u > m_d$, then these transition in ϕ_d are the minimal energy solutions and the ϕ_u solutions above become unstable. In reality $m_d > m_u$, and the transitions to $(\phi_u, \phi_d) = (\pm 2\pi, 0)$ are the only stable transitions.

The general case of Equations (24) cannot be solved analytically and we present the numerical solution of Equation (24) in Figure 3. In order to gain an intuitive understanding of this wall, we examine the solution in the limit $m_\pi \ll m_{\eta'}$. In this case, the last term of (24) dominates unless ϕ_S is very close to the vacuum states, $\phi_S \simeq 2\pi n$. Thus, the central structure of the ϕ_S field is governed by the differential equation:

$$\ddot{\phi}_S = \frac{8E}{N_c f_\pi^2} \sin\left(\frac{\phi_S}{N_c}\right). \quad (25)$$

Now, there is the issue of the cusp singularity when $\phi_S = \pi$ because we change from one branch of the potential to another as expressed in Equation (2). By definition, we keep the lowest energy branch, such that the right hand side of Equation (25) is understood to be the function $\sin(\frac{\phi_S}{N_c})$ for $0 \leq \phi_S \leq \pi$ and $\sin(\frac{\phi_S - 2\pi}{N_c})$ for $\pi \leq \phi_S \leq 2\pi$. However, we notice that the equations of motion are symmetric with respect to the center of the wall (which we take as $z = 0$), hence $\phi_S = \pi$ only at the center of the wall and not before, so we can simply look at half of the domain, $z \in (-\infty, 0]$, with boundary conditions $\phi_S = 0$ at $z = -\infty$ and $\phi_S = \pi$ at $z = 0$. The rest of the solution will be symmetric with $\phi_S = 2\pi$ at $z = +\infty$. Equation (25) with the boundary conditions above has the solution

$$\phi_S(z) \equiv (\phi_u(z) + \phi_d(z)) = \begin{cases} 4N_c \tan^{-1} \left[\tan\left(\frac{\pi}{4N_c}\right) \exp[\mu(z - z_0)] \right] & , \quad z \leq z_0 \\ 2\pi - 4N_c \tan^{-1} \left[\tan\left(\frac{\pi}{4N_c}\right) \exp[-\mu(z - z_0)] \right] & , \quad z \geq z_0 \end{cases} \quad (26)$$

where z_0 is the position of the center of the domain wall and

$$\mu \equiv \frac{2\sqrt{2}\sqrt{E}}{N_c f_\pi}, \quad \lim_{m_q \rightarrow 0} \mu = m_{\eta'} \quad (27)$$

is the inverse width of the wall, which is equal to the $m_{\eta'}$ mass in the chiral limit (see Equation (17)). Thus, we see that the dynamics of the central portion of QCD domain walls is governed by the η' field. We shall also refer to the ϕ_S transition (26) which occurs in several places (see for example Section III C 2) as the η' domain wall. The first derivative of the solution is continuous at $z = z_0$, but the second derivative exhibits a finite jump.

Before we continue our discussions regarding the structure of QCD domain walls, a short remark is in order: The sine-Gordon equation which is similar to Equation (25) with a cusp singularity, was first considered in [24] where a solution similar to (26) was presented. There is a fundamental difference, however, between domain walls discussed in [24] and the domain walls we consider here. In [24], the domain walls were constructed as auxiliary objects in order to describe a decay of metastable vacuum states which may exist under the certain circumstances. The walls we discuss here classically *stable* physical objects where the solutions interpolate between the same vacuum state; their existence is a consequence of the topology of the $U(1)$ singlet η' field. This topology, represented by the exact symmetry $\theta \equiv \theta + 2\pi n$ in Equation (2) is a very general property of QCD and does not depend on the specific choice of parameters or functional form of the effective potential. Similar equations and solutions with application to the axion physics were also discussed in [23].

The solution described above is dominates on scales where $|z| \leq \mu^{-1}$, however, the isotopical triplet pion transition can only have a structure on scales larger than $m_\pi^{-1} \gg \mu^{-1}$ and so the central structure of the η' wall can have little effect on the pion field. Indeed, we can see that, for $|z| \gg \mu^{-1}$, ϕ_S is approximately constant with the vacuum values. Making this approximation, we see that the isotopical triplet field is governed by the equation

$$\ddot{\phi}_T = 2m_\pi^2 \sin\left(\frac{\phi_T}{2}\right). \quad (28)$$

This has the same form as (25) and hence the solution is

$$\phi_T(z) \equiv (\phi_u(z) - \phi_d(z)) = \begin{cases} 8 \tan^{-1} \left[\tan\left(\frac{\pi}{8}\right) \exp[m_\pi(z - z_0)] \right], & -\infty < z - z_0 \ll -\mu^{-1} \\ 2\pi - 8 \tan^{-1} \left[\tan\left(\frac{\pi}{8}\right) \exp[-m_\pi(z - z_0)] \right], & \mu \ll z - z_0 < +\infty \end{cases} \quad (29)$$

which is a reasonable approximation for all z . Numerical solutions for the ϕ_S and ϕ_T fields are shown along with the same solution in terms of the ϕ_u and ϕ_d in Figure 3. As we can see from the explicit form of the presented solution, the η' transition is sandwiched in the pion transition. This is a key feature for some applications of this type of the domain wall as discussed in [7] for example.

The wall surface tension defined by Equation (19) can be easily calculated analytically in the chiral limit when the analytical solution is known and is given by Equations (26) and (29). Simple calculations leads to the following result⁵

⁵The N_c dependence displayed in Equation (30) corresponds to $\sigma \sim \sqrt{N_c}$ in large N_c limit. It is in variation with the arguments [22], [23] that in SYM as well as in pure gluodynamics, σ should be proportional to N_c while the wall's width scales as N_c^{-1} . Based on this observations, authors [22] argued that there should exist heavy glue states with masses $\sim N_c$ out of which the walls are built. Also, the same authors argued (see also [5]) that the heavy glue states cannot be integrated out—instead, they constitute a core of the domain wall. By integrating them out one produces cusp singularities in the low-energy effective Lagrangian, and the walls crossing the cusps cannot be studied consistently.

While we are not disputing the general arguments presented in [22,23,5], we would like to point out, that the large N_c counting may not be the best guide for certain kinds of delicate questions. For example, the π meson contribution to σ , which was ignored in Equation (30), has exactly required scaling properties with respect to N_c . Indeed, its contribution is proportional to $f_\pi^2 m_\pi$, which scales like N_c in large N_c limit rather than $\sqrt{N_c}$ that follows from Equation (30). However, numerically, the η' contribution is much more important. Besides that, the argument given in [22] for pure gluodynamics may not necessarily work for QCD with light quarks. Indeed, a pure gluonic operator $\frac{\alpha_s}{8\pi} G\tilde{G}$: is a perfect order parameter in gluodynamics, has an expected N_c behavior $\langle \theta | \frac{\alpha_s}{8\pi} G\tilde{G} | \theta \rangle \sim N_c$, changes the sign at $\theta = \pi$ when two gluonic vacua are degenerate in the course of interpolating θ from 0 to 2π , etc. At the same time, in QCD with light quarks, it vanishes in the chiral limit as the Ward identities require, but still has correct scaling properties $\sim N_c$ in the large N_c limit. Indeed, $\langle \theta | \frac{\alpha_s}{8\pi} G\tilde{G} | \theta \rangle = -m | \langle 0 | \bar{\Psi} \Psi | 0 \rangle | \sin \frac{\theta}{2} \sim N_c$, see (12).

To conclude this long footnote: we are not disputing the fact that, as large N_c arguments apparently suggest [22,5], the gluonic degrees of freedom may change the numerical estimates given below. The most important fact for what follows is this: QCD domain walls do exist. They are classically stable objects that become unstable on the quantum level. The relevant life-time is expressed entirely in terms of Λ_{QCD} , (see Section IV). Therefore, they are short-lived domain walls which are not cosmological disasters, but rather, may play an important role in evolution of the early universe. A precise calculation of their properties may require the knowledge of the dynamics of heavy degrees of freedom; however, for our the purposes of estimation, we ignore them in the present work.

$$\sigma = \frac{4N_c}{\sqrt{2}} f_\pi \sqrt{\langle \frac{b\alpha_s}{32\pi} G^2 \rangle} \left(1 - \cos \frac{\pi}{2N_c} \right) + O(m_q f_\pi^2). \quad (30)$$

In case when $m_q \neq 0$, an analytical solution is not known, but numerically, σ is close to the estimate (30).

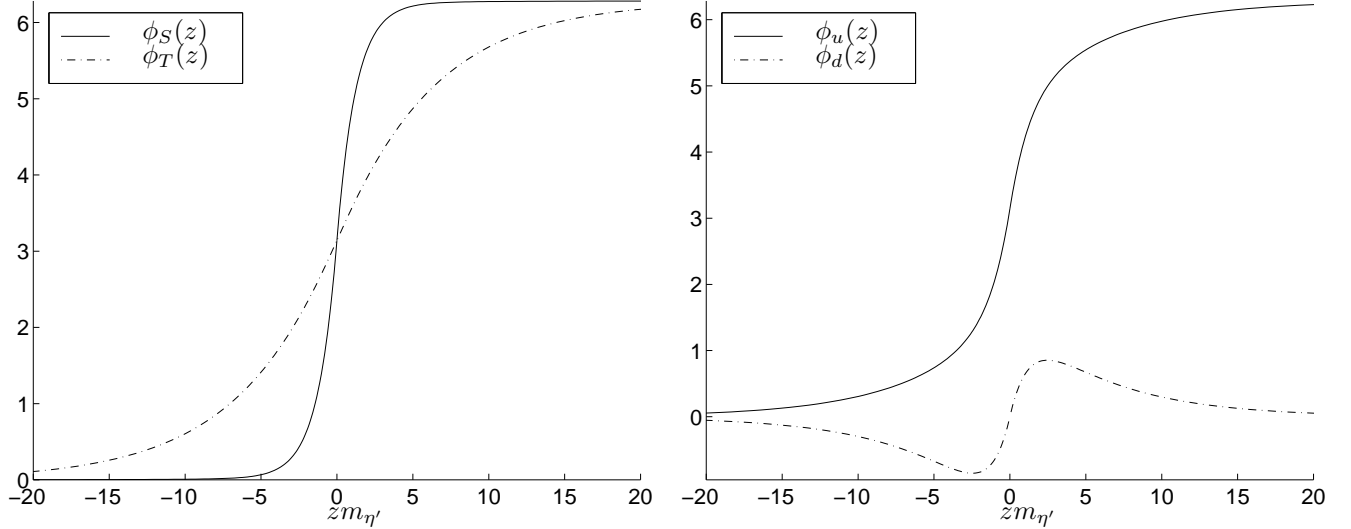


FIG. 3. Basic form of the QCD domain walls. Notice that the scale for the pion transition is larger than for the eta' transition. Notice that the width of the η' wall is set by the scale $m_{\eta'}$.

C. Axion Dominated Domain Walls

In the previous subsection when the QCD domain walls were discussed, the axion was not introduced as a dynamical field. In this subsection we assume that the axions exist. In this case there are domain walls in which the axion is the dominant player. The introduction of axions, in most cases, makes the domain wall an absolutely stable object. Our case is no exception and the axion model under discussion, (which is the $N = 2$ axion models according to the classification [21]) is an absolutely stable object. At the same time it is well-known [25,26], that stable domain walls can be a cosmological disaster. We do not address in this paper the problem of avoiding a domain wall dominated universe. Rather, we would like to describe some new elements in the structure of axion domain walls, which were not previously discussed.

The first and most natural type of the axion domain wall was discussed by Huang and Sikivie [27] who neglected the η' field in their construction. We shall refer to this wall as the Axion-Pion domain wall (a_π). As shown in [27], it has a width of the scale $\sim m_a^{-1} \gg \Lambda_{\text{QCD}}^{-1}$ for both the axion and π meson components. As Huang and Sikivie expected, the η' plays a very small role in this wall. In what follows we include a discussion of this type of domain wall for the completeness.

Our original result is to description a new type of the axion domain wall in which the η' field is a dominant player. We shall call this new solution the Axion-Eta' domain wall ($a_{\eta'}$). This new type of the domain wall was considered for the first time in [7] as a possible source for galactic magnetic fields in early universe. In what follows we give a detail description of the solution for the $a_{\eta'}$ wall. Here we want to mention the fundamental difference between the a_π wall discussed in [27] and the $a_{\eta'}$ wall introduced in [7]. Unlike the a_π wall which has structure only on the huge scale of m_a^{-1} , the $a_{\eta'}$ wall has nontrivial structure at both the axion scale m_a^{-1} as well as at the QCD scale $m_{\eta'}^{-1} \sim \Lambda_{\text{QCD}}^{-1}$. The reason for this is that, in the presence of the non-zero axion field (which is equivalent to a non-zero θ parameter), the pion mass is efficiently suppressed due to its Goldstone nature, thus the pion field follows the axion field and has a structure on the same m_a^{-1} scale. The η' , however, is not very sensitive to θ and so it remains massive. Again, the $a_{\eta'}$ solution has a sandwich structure with the singlet transition occurring at the center of the wall. One can adopt the viewpoint that the $a_{\eta'}$ domain wall is an axion domain wall with a QCD domain wall sandwiched in the center. This phenomenon is critical for applications involving the interaction of domain walls with strongly interacting particles. Indeed, there is no way for the a_π wall to trap any strongly interacting particles, like nucleons, because of the huge difference in scales; the $a_{\eta'}$ wall, however, has a QCD structure and can therefore efficiently interact with nucleons on the QCD scale $\Lambda_{\text{QCD}}^{-1}$. Regarding the wall tension (19), it is dominated by the axion physics and thus has the same

order of magnitude for both types of the axion domain walls which is proportional to $\sigma \sim \frac{M}{m_a} \sim f_a f_\pi m_\pi$ as found in [27].

1. Axion-Pion Domain Wall

The solution discussed by Huang and Sikivie corresponds to the transition $(a, \phi_u, \phi_d) : (0, 0, 0) \rightarrow (\pi, \pi, -\pi)$, i.e., by a transition in the axion and pion fields only. This transition describes the a_π wall. Indeed, in terms of (a, ϕ_S, ϕ_T) this transition corresponds to a nontrivial behavior of the axion and triplet pion component ϕ_T of the ϕ_u, ϕ_d fields: $(a, \phi_S, \phi_T) : (0, 0, 0) \rightarrow (\pi, 0, 2\pi)$. The other transition (the $a_{\eta'}$ wall) corresponds to the transition $(a, \phi_u, \phi_d) : (0, 0, 0) \rightarrow (-\pi, \pi, \pi)$ in which the singlet η' field is dominant: $(a, \phi_S, \phi_T) : (0, 0, 0) \rightarrow (-\pi, 2\pi, 0)$. It will be considered later on.

Huang and Sikivie discussed the solution to this wall in the limit where the η' field is extremely massive and hence they neglected its role. It can be integrated out which effectively corresponds to fixing it $\eta'(z) = 0$. Indeed, if we simply fix $\eta'(z) = 0$ in our equations, then we reproduce their solution. When E is large, then $m_\pi \ll m'_\eta$ as Huang and Sikivie assumed, the effects of the η' particle can be neglected and the solution for the the axion and pion fields presented in [27] is valid for the boundary conditions described above. We plot this numerical solution which includes the η' effects in Figure 4. As announced above, the a_π solution has the only scale of $\sim m_a^{-1}$ for both components, axion as well as the pion field $\sim \phi_T$. The η' field remains close to the its vacuum value and only slightly corrects the solution.

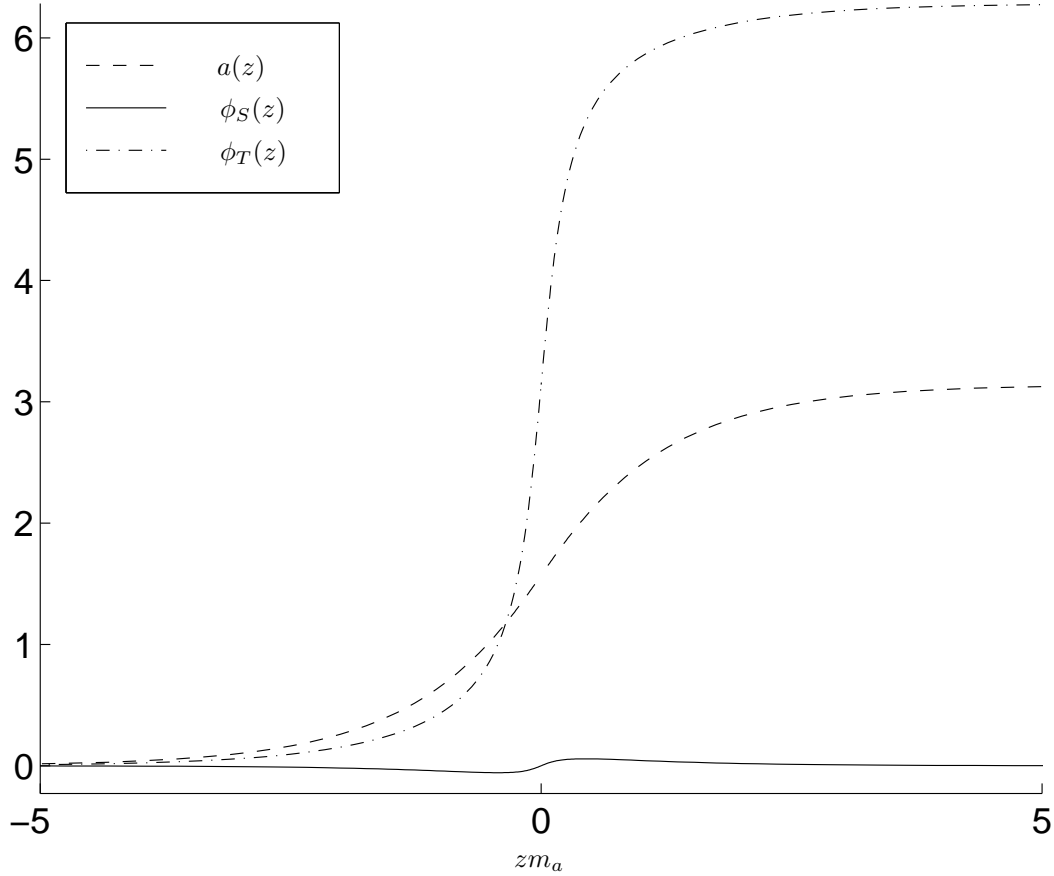


FIG. 4. Basic form of the a_π domain wall. Notice that all the fields have a structure on the scale of m_a^{-1} and that the isotopical singlet fields plays a very small role.

Having looked at the solution of the a_π wall, we now investigate the structure of the $a_{\eta'}$ domain wall which is a new solution. This solution corresponds to the transition $(a, \phi_u, \phi_d) : (0, 0, 0) \rightarrow (\pi, \pi, \pi)$. Now the singlet η' field undergoes a transition instead of the triplet pion field: $(a, \phi_S, \phi_T) : (0, 0, 0) \rightarrow (-\pi, 2\pi, 0)$. As we discussed above, the singlet field never becomes massless, and therefore, a new structure at the QCD scale $\sim \Lambda_{\text{QCD}}^{-1}$ emerges in sharp contrast to the well-studied a_π domain wall [27] where no such structure appears. We should note that the potential (20) has the same vacuum energy at $\phi_S = 0$ as well as at $\phi_S = 2\pi$ due to the change of ϕ_S field to the lowest energy branch at $\phi_S = \pi$ as described by Equation (2). Therefore, this domain wall interpolates between two degenerate states, and thus, like the a_π domain wall [27], the solution under these considerations is absolutely stable.

For $|z| \gg \mu^{-1}$, the last term in (23) is negligible and so the solution behaves like the a_π wall. What happens is that, away from the wall, the axion field dominates and shapes the wall as it does in with the a_π solution. Again, the pion mass is suppressed and $\phi_S \approx 0$. As $z \sim \mu^{-1}$ however, the last term of (24) starts to dominate the behaviour. At this point, the $a_{\eta'}$ wall undergoes a sharp transition similar to the QCD domain wall described by (26). We plot this solution along with a blowup in Figure (5). Notice also, that the singlet field cancels the effects of the axion near the center of the wall, and so the pion field becomes massive again as it undergoes its transition.

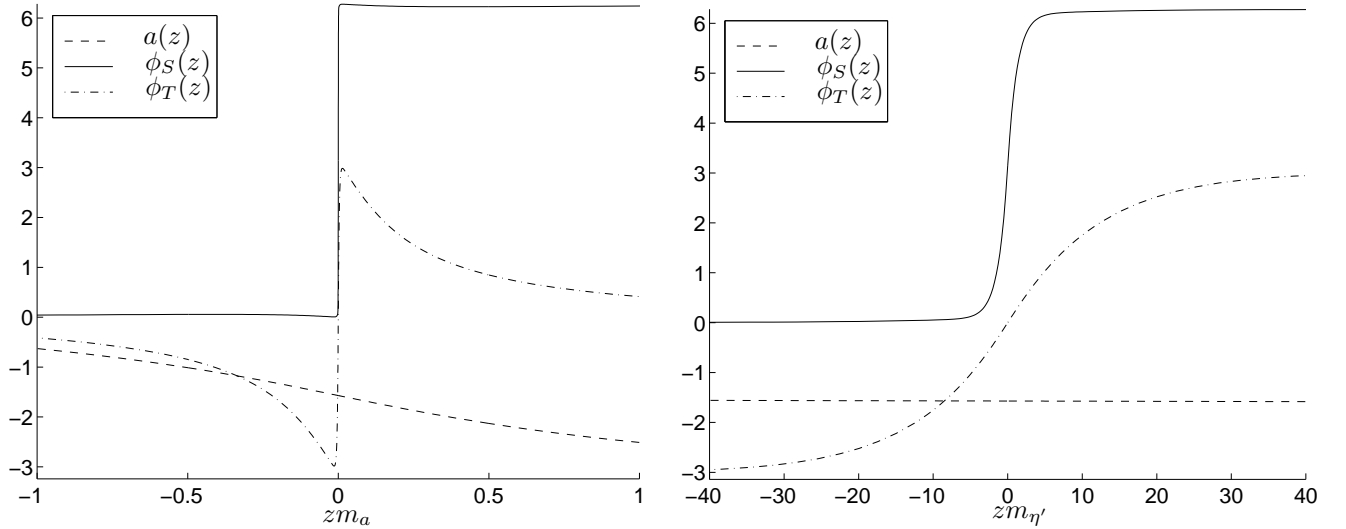


FIG. 5. Basic form of the $a_{\eta'}$ domain walls with a closeup where the axion field $a \approx \pi/2$. Notice that the large scale structure is similar to that of the a_π wall, but that there is also a small scale structure on the scale of $m_{\eta'}$. Near the center of the wall, the pion regains its mass and undergoes a transition on the scale of m_π .

IV. DECAY OF THE QCD DOMAIN WALLS

Up to this moment, we have treated the domain walls as topologically stable objects. We do not have much new to say regarding the stability for general types of the domain walls, nor do we have a resolution for the general problem of avoiding a domain wall dominated universe. We refer to the nice text book [26] for the references on the subject. Instead, this section is devoted specifically to the QCD domain walls discussed in Section III B. Here we argue that QCD domain walls (not the axion walls) are unstable on the quantum level due to tunneling. We estimate the relevant life-time of this quantum transition which turns out to be quite short on the cosmological scale but quite long with respect to the QCD scale $\Lambda_{\text{QCD}}^{-1}$ albeit it is exponentially suppressed as it should be. Therefore, these walls do not pose a cosmological problem as one might naïvely suspect⁶. We have nothing new to say regarding the stability or

⁶We should remind the reader once again that the existence of the QCD domain walls described above is the reflection of the well-understood symmetry $\theta \rightarrow \theta + 2\pi n$ and, is the consequence of the topological charge quantization; their existence is not based on any model-dependent assumptions we have made to support the specific calculations in the previous sections.

evolution of axion domain walls [28,29] (which were also discussed in the previous sections), see [30] and references therein for a recent review on the subject.

Having said that the QCD domain walls are unstable, a very natural question occurs: “What sense does it make to study an object which does not presently exist?” The answer is: “It does not make much sense if we study QCD at the present cosmological epoch. However, if we want to understand what happened shortly after the QCD phase transition in the evolution of the early universe, or what may happen at RHIC after the transition from a quark-gluon plasma to the hadronic phase when system cools, then this is perfectly reasonable question to ask (and hopefully answer!)” Indeed, according to the standard theory of the cosmological phase transitions [31,26], if, below a critical temperature T_c , the potential develops a number of degenerate minima, then the choice of minima will depend on random fluctuations in fields. The minima that the fields settle to can be expected to differ in various regions space. If neighboring volumes fall into different minima, then a kink (domain wall) will form as a boundary between them.

For the present estimate of the decay rate for the QCD domain wall, the only information we need from the previous sections are: the domain wall tension σ and the wall thickness. In the chiral limit for two light flavors $N_f = 2$, the tension σ is given by Equation (30) which we would like to present in the following form:

$$\sigma = \frac{4N_c f_\pi \sqrt{E}}{\sqrt{2}} \left(1 - \cos \frac{\pi}{2N_c} \right), \quad (31)$$

In this formula, the $\sqrt{2}$ in denominator should be replaced by $\sqrt{N_f}$ for an arbitrary N_f ; however in all numerical estimates we shall use $N_f = 2$ which we believe is very good approximation for our problem in the limit $m_u \simeq m_d \ll m_s$ as Equations (10) and (11) suggest. Besides that, for $N_c \geq 3$, one can approximate $1 - \cos[\pi/(2N_c)] \simeq \pi^2/(8N_c^2)$ such that Equation (31) takes especially simple form which will be used in the numerical estimates which follow,

$$\sigma = \frac{\pi^2 f_\pi \sqrt{E}}{2\sqrt{2}N_c} \simeq (200 \text{ MeV})^3. \quad (32)$$

What to use as the wall thickness is a more subtle question due to the “sandwich structure” of the QCD domain walls described above. As we discussed in the previous sections, the core of the QCD domain wall is determined by the flavour isotopical singlet η' field with thickness $\mu^{-1} \simeq m_{\eta'}^{-1}$, while the π meson halo has a much larger size $\sim m_\pi^{-1}$. Nevertheless, in what follows we treat the QCD domain wall as the object with wall thickness of order $\sim m_{\eta'}^{-1}$ due to the fact that the most important contribution to σ comes from this small region of $\Delta z \sim m_{\eta'}^{-1}$. Indeed, as Equation (19) suggests, the contribution to σ from the η' field is proportional to $E\Delta z \sim E/m_{\eta'}$. At the same time, the contribution to σ from the π field, which was ignored in (31) and (32), is proportional to $m_q \langle \bar{\Psi}\Psi \rangle \Delta z \sim m_q \langle \bar{\Psi}\Psi \rangle / m_\pi \sim m_\pi \rightarrow 0$ which vanishes in the chiral limit. Therefore, despite of the fact that the π meson cloud is of a much larger in size, its contribution to σ is much smaller, as announced earlier. Numerically, the π contribution consists only 10% of σ and we ignore this contribution in what follows.

We are now prepared to discuss the decay of the QCD domain walls. The decay mechanism is due to a tunneling process which creates a hole in the domain wall. This hole connects the configurations $(\phi_u, \phi_d) = (0, 0)$ to the $(\phi_u, \phi_d) = (2\pi, 0)$ domain (see Equation (11)). This decay mechanism is similar to the decay of a metastable wall bounded by strings, and we use a similar technique to estimate the tunneling probability. In this case, the walls can decay by quantum nucleation of holes which are bounded by strings. The idea of the calculation was suggested by Kibble [32], and has been used many times since then (see the textbook [26] for a review). The most well known example of such a calculation is the calculations of the decay rate in the so-called $N_{PQ} = 1$ axion model where the axion domain wall become unstable for a similar reason due to the presence of axion strings [29,30]. However, as was emphasized in [33], the existence of strings as the solutions to the classical equations of motion is not essential for this decay mechanism (see below). Some configurations, not necessarily the solutions of classical equations of motion, which satisfy appropriate boundary conditions, may play the role played by strings in the $N_{PQ} = 1$ axion model.

To be more specific, let us consider a closed path starting in the first domain with $(\phi_u, \phi_d) = (0, 0)$, which goes through the hole and finally returns back to the starting point by crossing the wall somewhere far away from the hole. The phase change along the path is clearly equals to $\phi_u + \phi_d = 2\pi$. Therefore, the absolute value of a field which gives the mass to the η' field (the dominant part of the domain wall) has to vanish at some point inside the region encircled by the path. By moving the path around the hole continuously, one can convince oneself that there is a loop of a string-like configuration (where the absolute value of a relevant field vanishes such that the η' singlet phase is a well defined) enclosing the hole somewhere. In this consideration we did not assume that a hole, or string enclosing

the hole, are solutions of the equations of motion⁷. They do not have to be solutions.

However, if we want to describe the hole nucleation semi-classically [32,26], then we should look for a corresponding instanton which is a solution of Euclidean (imaginary time, $t = i\tau$) field equations, approaching the unperturbed wall solution at $\tau \rightarrow \pm\infty$. In this case the probability P of creating a hole with radius R per area S per time T can be estimated as follows⁸ [32,34,35]:

$$\frac{P}{ST} \sim \left[\sqrt{\frac{S_0}{2\pi}} \right]^3 e^{-S_0} \times \text{Det}, \quad (33)$$

where S_0 is the classical instanton action; Det can be calculated by analyzing small perturbations (non-zero modes contribution) about the instanton, (see [35] for an explanation of the meaning of this term) and will be estimated using dimensional arguments; and $(\sqrt{S_0/(2\pi)})^3$ is the contribution due to three zero modes describing the instanton position⁹.

If the radius (a critical radius R_c to be estimated later) of the nucleating hole is much greater than the wall thickness, we can use the thin-string and thin-wall approximation, in this case, the action for the string and for the wall are proportional to the corresponding worldsheet areas [32],

$$S_0 = 4\pi R^2 \alpha - \frac{4\pi}{3} R^3 \sigma. \quad (34)$$

Here σ is the wall tension (32), and α is the string tension, to be estimated. The world sheet of a static wall lying in the x - y plane is the three-dimensional hyperplane $z = 0$. In the instanton solution, this hyperplane has a “hole” which is bounded by the closed worldsheet of the string. Minimizing (34) with respect to R we find that

$$R_c = \frac{2\alpha}{\sigma}, \quad S_0 = \frac{16\pi\alpha^3}{3\sigma^2}. \quad (35)$$

The Lorentzian evolution of the hole after nucleation can be found by making the inverse replacement $\tau \rightarrow -it$ from Euclidean to Minkowski space-time. The hole expands with time as $x^2 + y^2 = R^2 + t^2$, rapidly approaching the speed of light.

Now we want to estimate the string tension α . As we mentioned above (see footnote 7), we cannot make this estimate with Equation (2) where the gluon degrees of freedom are integrated out and replaced by their vacuum expectation values. Instead, we have to take one step back and consider the original Lagrangian [10] which includes the complex gluon degrees of freedom h :

$$V(\theta, h, U) = \left(\frac{1}{4} \frac{1}{N_c} h \log \left[\left(\frac{h}{2eE} \right)^{N_c} \frac{\text{Det } U}{e^{-i\theta}} \right] - \frac{1}{2} \text{Tr } MU \right) + \text{h.c.} \quad (36)$$

This satisfies all the conformal and chiral anomalous Ward identities, has the correct large N_c behaviour etc. (see [10,24] for details). Integrating out the heavy h field will bring us back to Equation (2). It is interesting to note that the structure of Equation (36) is quite similar in structure to the effective potential for SQCD [9] and gluodynamics [37].

⁷It is quite obvious that such a configuration cannot be described within our non-linear σ model given by Equation (2) where it was assumed that the gluon as well as the chiral condensates are non-zero constants. In this case, the singlet phase is not well defined everywhere. However, in the case of a triplet π meson string, such a configuration can easily be constructed within a linear σ model by allowing the absolute value of the chiral condensate to fluctuate along with the Goldstone phase (π meson field). The σ term in the linear σ model essentially describes the rigidity of the potential. Indeed, the corresponding calculations within a linear σ model were carried out in [36] where it was demonstrated that the solution describing the π meson string exists, albeit unstable as expected from the topological arguments. To carry out a similar calculations in our case for the singlet η' phase, one should allow fluctuations of the gluon fields: the fields that give mass to η' meson and that describe the rigidity of the relevant potential (see below).

⁸The estimate given below is designed for illustrative purposes only, and should be considered as a very rough estimation of the effect to an accuracy not better than the order of magnitude.

⁹The three zero modes in our case should be compared with the four zero modes from the calculations of [34,35]. This difference is due to the fact that in [34,35] the decay of three dimensional metastable vacuum state was discussed. In our case, we discuss a decay of a two-dimensional object.

Let us stop for a moment to consider the form of this potential. When we integrate out the heavy gluon degrees of freedom, we replace h with its vacuum expectation value $\langle h \rangle$. The vacuum expectation value¹⁰ of the h is given by

$$\langle h \rangle = 2E \exp(-i \sum \phi_i / N_c) \quad (37)$$

such that (36) becomes

$$V(U)|_{\theta=0, h=\langle h \rangle} = -E \cos\left(\frac{1}{N_c} \sum \phi_i\right) - \sum M_i \cos \phi_i, \quad (38)$$

in agreement with (8). With h fixed at its vacuum expectation value, the singlet combination $\phi_S = \sum \phi_i$ exhibits the $U(1)$ topology described above and our domain walls are stable. Now, however, we consider $h = \rho \langle h \rangle$ where ρ is a real physical fields related to glueballs. In this case, the potential V is given by

$$V(\rho, \phi_S) = +E\rho(\log \rho - 1) \cos \frac{\phi_S}{N_c} \quad (39)$$

where we have neglected the terms proportional to M as they are negligible since they only contribute a constant offset due to the ϕ_T field. For an early phenomenological discussion of the potential (39) without the ϕ_S fields, see [38].

Now the combined degrees of freedom ρ and ϕ_S are no longer restricted to the circle $\rho = 1$ as they were in the effective theory (2). The $U(1)$ topology is no longer a constraint of the fields and thus, the walls are not topologically stable. Instead, the restriction of $\rho \approx 1$ is dynamical, and made by a barrier at $h = 0$. Thus, with these degrees of freedom, the fields parameterize the plane, however, the potential is that of a tilted Mexican hat with a barrier at $h = 0$. The barrier is high enough that a domain wall interpolating around the trough of the hat is classically stable. If the barrier were infinitely high as we assumed when we fixed $\rho = 1$ as we did in (2), then the ϕ_S field could wind around the barrier and would be topologically stable. With a finite barrier, however, the field can tunnel through the barrier as described above. This situation is analogous to the case of the string and peg shown in Figure 2. We show a more accurate picture of the barrier (39) in Figure 6.

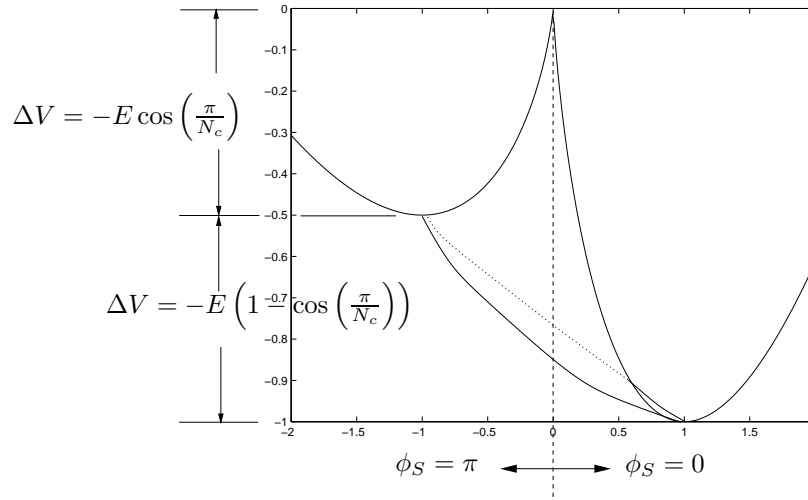


FIG. 6. Profile of the “Mexican hat” potential (39). The slice is made along the axis through $\phi_S = \pi$ to the left and $\phi_S = 0$ to the right. The trough of the potential lowers from the cusp at $\rho = 1$, $\phi = \pi$ where $V = -E \cos(\frac{\pi}{N_c})$ down to the vacuum state $V_{\min} = -E$. The hump where $V = 0$ is at the origin is where $h = \rho \exp(i\phi_S/N_c) = 0$ and hence the singlet field ϕ_S can have any value at this point. It is by passing across this point that a QCD domain wall can tunnel and a hole can form.

¹⁰For more accurate treatment of the minimization procedure which carefully accounts for the different branches, see the original paper [24].

The most important property of the potential is the following: The absolute minimum of the potential in the chiral limit corresponds to the value $V_{\min} = -E$ which is the ground state of our world with $\rho = 1$ and $\phi_s = 0$. At the same time, the maximum of the potential (2), where one branch changes to another one is $V = -E \cos(\pi/N_c)$ where $\phi_s = \pi$ (we are still taking $\theta = 0$). This corresponds to the point $\rho = 1$ and $\phi_s = \pi$ in the potential (39). Thus, the trough of the Mexican hat is given where $h = \langle h \rangle$, ie. at radius $\rho = 1$ and the maximum $V = -E \cos(\pi/N_c)$ of the potential (2) is exactly the barrier through which the η' field interpolate to form the QCD domain wall. It is important to note that the height of the barrier for the potential (2) is numerically is quite high $\sim E(1 - \cos \frac{\pi}{N_c})$, but that vanishes in large N_c limit. Indeed, in this limit, the peak of the barrier is degenerate with the absolute minimum $V_{\min} = -E$ of the potential as it should be¹¹. The height of this barrier describes how much the Mexican hat it tilted.

The other important property of the potential (39) is its value where the singlet phase $\sum \phi_i$ is well defined. From (39) it is clear that this occurs when $h = 0$. This is exactly the height of the peak of the Mexican hat (or the peg in Figure 2) which classically prevents $\rho \rightarrow 0$ and which makes the QCD domain wall classically stable. The energetic barrier at $h = 0$ that tells us the energetic cost to create the “string” around the edge of the hole which must accompany the hole, and which includes the region with $h = 0$. Potential (39) vanishes at this point, $V(h = 0) = 0$, which implies that the barrier at $h = 0$ is quite high: $\Delta V = E$. As expected, the barrier at $h = 0$ should be order of $E \sim N_c^2$ in contrast with the barrier to η' where one should expect a suppression by some power of N_c . We also note that the total number of classically stable solutions can be estimated from the condition $\cos(\pi k/N_c) > 0$ where the barrier for the η' field is still lower than the peak $h = 0$. Thus, $-N_c/2 < k < N_c/2$ where k labels the solutions.

As a consequence, we estimate the string tension α using pure dimensional arguments: $\alpha \sim \sqrt{2E}$ where $2E$ is the only relevant dimensional parameter of the problem in the chiral limit. This parameter enters Equation (36) such that $\langle h \rangle = 2E$. Therefore¹²,

$$\alpha \simeq \sqrt{2E} \sim (0.28 \text{ GeV})^2, \quad R_c = \frac{2\alpha}{\sigma} \sim \frac{8N_c}{\pi^2 f_\pi} \sim \frac{2.4}{f_\pi}, \quad S_0 = \frac{16\pi\alpha^3}{3\sigma^2} \sim \frac{256N_c^2 \sqrt{2E}}{3\pi^3 f_\pi^2} \sim (110 - 140), \quad (40)$$

where the uncertainty in S_0 reflects a 10% variation in α from the central value given in (40). Of course, a more realistic error in estimate (40) would be much higher. It is quite remarkable: in spite of the fact that all parameters in our problem are QCD parameters of order Λ_{QCD} , the classical action S_0 could be numerically quite large, and thus the corresponding probability (33) may be quite small. We do not see any simple explanation for this phenomenon except for the fact that expressions (34) and (40) for S_0 contains a huge numerical factor $\frac{16\pi}{3}$ of purely geometrical origin. In addition, since $S_0 \sim N_c^2$, one should expect an additional enhancement in S_0 .

Here we mention an interesting note: As we mentioned earlier, in QCD there is only one dimensional parameter, Λ_{QCD} , and it is thus generally believed that the semi-classical approximation in QCD cannot be parametrically justified. Nevertheless, numerically R_c is quite large, much larger than the width μ^{-1} of the domain wall (27) which is essentially set by $m_{\eta'}^{-1}$. Therefore, the semi-classical approximation (33) is somewhat justified a posteriori.

Now, we are prepared to make our last step and estimate the probability of creating a hole with radius $R_c \sim \frac{8N_c}{\pi^2 f_\pi}$:

$$\frac{P}{T} \sim \pi R_c^2 \left[\sqrt{\frac{S_0}{2\pi}} \right]^3 e^{-S_0} \times \text{Det} \sim \pi R_c^2 E^{\frac{3}{4}} \left[\sqrt{\frac{S_0}{2\pi}} \right]^3 e^{-S_0}. \quad (41)$$

We have estimated $\text{Det} \sim E^{\frac{3}{4}}$ through dimensional analysis. Using the numerical values given above for R_c and $S_0 \simeq 130$ we arrive to the following final result:

$$\frac{P}{T} \sim \sim 10^3 e^{-130} \text{ GeV} \sim 10^{-30} s^{-1}. \quad (42)$$

The most amazing result of the estimate (42) is the astonishingly small probability for the decay $P \sim 10^{-50} \text{ GeV}$ which one might naïvely expect to be on the GeV level. This small number leads to a very large life time for the domain walls, and consequently, makes them relevant to cosmology at the QCD scale. Of course, our estimation of

¹¹Remember, the η' direction becomes flat in the large N_c limit as $m_{\eta'} \rightarrow 0$.

¹²The magnitude for $\alpha \sim \sqrt{2E} \sim (0.28 \text{ GeV})^2$ should not be considered as a strong overestimation; rather it should be considered as a lower bound. Indeed, if one considers the π meson string [36] which should be much softer (and therefore, would possess much smaller α_π) one finds, nevertheless, that $\alpha_\pi \simeq \pi f_\pi^2$ is very close numerically to our estimation for the η' string tension.

S_0 is not robust, and even small variation of parameters may drastically change our estimate (42), making it much larger or much smaller. In what follows we stick with estimate (42) for cosmological applications.

First of all, let us estimate an average size l of a domain wall before it collapses with an average lifetime of $\tau_l \sim l/c$. This corresponds the situation when the probability of the decay is close to one. If L is the Hubble size scale, $L \sim 30$ km, then

$$P \simeq \frac{P}{T} \cdot \frac{l^2}{\pi R_c^2} \cdot \tau_l \sim \frac{P}{T} \cdot \frac{L^2}{\pi R_c^2} \cdot \frac{L}{c} \cdot \left(\frac{l}{L}\right)^3 \sim 10^{-30} s^{-1} \cdot 10^{36} \cdot 10^{-4} s \cdot \left(\frac{l}{L}\right)^3 \sim 10^2 \left(\frac{l}{L}\right)^3 \simeq 1. \quad (43)$$

Formula (43) implies that the average size l of the domain wall before it collapses could be as large as the Hubble size $l \simeq 10^{-2/3} \cdot L \sim 0.2L$. It also implies that on a Hubble scale domain wall L , the average number of holes which will be formed is approximately $\langle n \rangle \sim (L/l)^2 \sim 25$. Finally, the lifetime of a Hubble size domain wall is expected to be on the scale of

$$\tau_l \sim \frac{L}{\sqrt{\langle n \rangle} c} \sim 2 \cdot 10^{-5} s, \quad (44)$$

which is macroscopically large!

It is clear that all these phenomena are due to the astonishingly small number (42) which makes the link between QCD and cosmology feasible. This small number is due to the tunneling process rather than some special fine-tuning arrangements. As we mentioned above, we have not made any adjustments to the phenomenological parameters used in the estimates. Rather, we have used the standard set of parameters introduced in Equation (2). To conclude the discussion of (42) we would like to remind the reader that similar miracles related to tunneling processes happens in physics quite often. For example, the difference in life time for U^{238} and Po^{212} under α decay is on the order of 10^{20} in spite of the fact that the “internal” physics of these nuclei, and all internal scales are very similar.

V. CONCLUSION AND FUTURE DIRECTIONS

The main results of this paper is expressed by the formulae (26) and (42) where a new type of a quasi-stable QCD matter—the QCD domain wall (which could have a macroscopically large size!)—is described. The lifetime (42) of the QCD domain walls is estimated to be very large, thus, such objects might play an important role on the evolution of the early universe soon after the QCD phase transition. See [7] for a first attempt in this direction.

One should emphasize also, that the interaction of the domain wall with nucleons can drastically change the properties of the domain wall due to the strong interaction of all relevant fields. In particular, the domain walls may become much more stable in the presence of nucleons, and even account for the strong self-interacting dark matter discussed in [39]. Future study will show whether or not this could be the case.

It would be very exciting if QCD domain walls can be studied at RHIC (Relativistic Heavy Ion Collider) [40]. Such a research would be the first experimental attempt to directly study the fundamental properties of the QCD vacuum structure.

As a by-product of our analysis, we also found a new type of the axion domain wall ($a_{\eta'}$) with a sandwich structure and which might be an interesting feature for further cosmological applications [7] if the axions exist.

VI. ACKNOWLEDGMENTS

This work is supported in part by the National Science and Engineering Research Council of Canada. AZ wishes to thank Misha Stephanov and Edward Shuryak for valuable comments and very useful discussions regarding the possibility of studying QCD domain walls at RHIC. He is also grateful to Paul Stenhardt for explaining his works [39] and for discussions of possibility of QCD domain walls as a strongly interacting dark matter candidate and thanks G. Dvali, G. Gabadadze and M. Shifman for useful discussions. AZ is also grateful to Larry McLerran for organizing a Russian style seminar where a speaker has no chance to respond to questions and critique.

[1] A. M. Polyakov, Nucl. Phys. **B120** (1977) 429.

- [2] N. Seiberg and E. Witten, Nucl. Phys. **B426** (1994) 19; Nucl. Phys. **B431** (1994) 484.
- [3] G't Hooft, in Confinement, Duality and Nonperturbative Aspects of QCD, P. van Baal, Ed, NATO ASI Series, 1998 Plenum Press, NY 1998; G't Hooft, hep-ph/9812204.
- [4] K. Konishi, and H.Terao Nucl. Phys. **B511** (1998) 264.
- [5] M. Shifman, Progr. Part. Nucl. Phys. **39** (1997) 1.
- [6] E. Witten, JHEP **9807** (1998) 6; Phys. Rev. Lett. **81**, 2862 (1998).
- [7] M.Forbes and A. Zhitnitsky, hep-ph/0004051
- [8] G. Veneziano and S. Yankielowicz, Phys. Lett. **113B** (1982) 231.
- [9] T. Taylor, G. Veneziano and S. Yankielowicz, Nucl. Phys. **B218** (1983) 439.
- [10] I. Halperin and A. Zhitnitsky, Phys. Rev. Lett. **81**, 4071 (1998); Phys. Rev. **D58**, 054016 (1998), hep-ph/9711398;
- [11] E. Witten, Ann. Phys. **128** (1980) 363.
P. Di Vecchia and G. Veneziano, Nucl. Phys. **B171** (1980) 253.
- [12] A.Kovner and M.Shifman, Phys. Rev. **D56** (1997) 2396.
- [13] V.A. Novikov, M.A. Shifman, A.I. Vainshtein and V.I. Zakharov, Nucl. Phys. **B191** (1981) 301.
- [14] R.J. Crewther, Phys. Lett. **70B** (1977) 349.
M.A. Shifman, A.I. Vainshtein, and V.I. Zakharov, Nucl. Phys. **B166** (1980) 493.
- [15] G. Veneziano, Nucl. Phys. **B159** (1979) 213.
- [16] R.Jackiw and C. Rebbi, Phys. Rev. Lett. **37** (1976) 172,
C.Callan, R.Dashen and D.Gross, Phys. Lett. **B 63** (1976) 334, Phys. Rev. **D17** (1978) 2717, 2763.
- [17] R. Peccei and H. Quinn, Phys. Rev. Lett. **38** (1977) 1440
- [18] S. Weinberg, Phys. Rev. Lett. **40** (1978) 223;
F. Wilczek, Phys. Rev. Lett. **40** (1978) 279.
- [19] J.E. Kim, Phys. Rev. Lett. **43** (1979) 103;
M.A. Shifman, A.I. Vainshtein, and V.I. Zakharov, Nucl. Phys. **B166** (1980) 493.
- [20] M. Dine, W. Fischler, and M. Srednicki, Phys. Lett. **B104** (1981) 199;
A.R. Zhitnitsky, Yad.Fiz. **31** (1980) 497 (Sov. J. Nucl. Phys. **31** (1980) 260).
- [21] J.E. Kim, Phys. Rep. **150** (1987) 1;
H.Y. Cheng, Phys. Rep. **158** (1988) 1;
R.D. Peccei, in "CP violation", ed. C. Jarlskog, World Scientific, Singapore, 1989.
- [22] G.Dvali, G. Gabadadze, Z. Kakushadze, Nucl. Phys. **B562** (1999) 158;
I. Kogan, A. Kovner, M.Shifman, Phys. Rev. **D57** (1998) 5195, hep-th/9712046.
M.Shifman, Phys. Rev. **D59** (1999) 021501, hep-th/9809184.
G. Gabadadze and M.Shifman, Phys. Rev. **D61** (2000) 075014, hep-ph/9910050.
- [23] G. Gabadadze and M.Shifman, hep-ph/0007345.
- [24] T. Fugleberg, I. Halperin and A. Zhitnitsky, hep-ph/9808469, Phys. Rev. **D59** (1999) 074023.
- [25] Ya.B.Zeldovich, I.Yu.Kobzarev and L.B.Okun, Sov. Phys.JETP **40** (1975)1.
- [26] A. Vilenkin, E. P. S. Shellard, Cosmic Strings and other topological defects, Cambridge University Press 1994.
- [27] M. C. Huang and P. Sikivie, Phys. Rev. **D32**, 1560 (1985).
- [28] P.Sikivie, Phys. Rev. Lett. **48** (1982) 1156;
A. Vilenkin and A. Everett, Phys. Rev. Lett. **48** (1982) 1867;
D. Lyth and E. Stewart, Phys. Rev. **D 46** (1992) 532.
- [29] R. Davis, Phys. Rev. **D 32** (1985) 3172; R. Davis and E. P. S. Shellard, Nucl. Phys. **B 324** (1989), 167;
E. P. S. Shellard and R. A. Battye, astro-ph/9802216,
D.Harari and P. Sikivie, Phys. Lett. **B195**, (1987) 361;
C.Hagmann and P. Sikivie, Nucl. Phys. **B 363** (1991) 247.
- [30] S. Chang, C. Hagmann, and P. Sikivie, Phys. Rev. **D59**, 023505 (1999).
- [31] T.W.B. Kibble, J.Phys. **A9** (1976) 1387.
- [32] T.W.B. Kibble, G.Lazarides and Q.Shafi, Phys. Rev. **D 26** (1982) 435.
- [33] G.Dvali et al, hep-ph/9411387
- [34] M.B. Voloshin, I.Yu. Kobzarev and L.B. Okun, Sov. J. Nucl. Phys. **20** (1975) 644.
- [35] S. Coleman, Phys. Rev. **D15**(1977) 2929.
- [36] R. Brandenberger and X.Zhang, Phys. Rev. **D59**(1999) 081301
- [37] A. A. Migdal and M. A. Shifman, Phys. Lett. **B114**, 445 (1982).
- [38] R. Gomm, P. Jain, R. Johnson and J. Schechter, Phys. Rev. **D33**, 801 (1986).
- [39] D.N.Spergel and P. Steinhardt, astro-ph/9909386,
B.Wandelt et al, astro-ph/0006344
- [40] M.Stephanov, E. Shuryak, A. Zhitnitsky, work in progress.